


Johannes Leipold<sup>1,\*</sup>  
Magnus Jung<sup>2</sup>  
Tobias Keßler<sup>1</sup>  
Achim Kienle<sup>1,2</sup>

# Nonlinear Behavior of Methanol Synthesis Compared to CO<sub>2</sub> Methanation

The nonlinear behavior of CO<sub>2</sub> methanation over a Ni-catalyst is compared to methanol synthesis over a standard Cu/ZnO-catalyst in a continuous stirred tank reactor (CSTR). Both reactions have received a lot of attention these days for chemical energy storage. Both reactions are exothermic but behave in a different way. CO<sub>2</sub> methanation is known to be strongly exothermic, giving rise to multiple steady states. This behavior is induced by the self-acceleration of the methanation reaction because the heat production of the chemical reaction increases with rising temperature. It is shown that methanol synthesis behaves fundamentally different under the operating conditions usually employed in practice. It is less exothermic but, even more important, the overall heat production of the methanol reaction system decreases with increasing temperature, giving rise to a unique and stable steady state. This insight is obtained with an extension of the classical graphical analysis with heat production and heat removal curves.

 This is an open access article under the terms of the Creative Commons Attribution-NonCommercial-NoDerivs License, which permits use and distribution in any medium, provided the original work is properly cited, the use is non-commercial and no modifications or adaptations are made.

**Keywords:** Bifurcation, Methane synthesis, Methanol synthesis, Multiple steady states, Sabatier reaction

*Received:* May 26, 2023; *revised:* October 30, 2023; *accepted:* October 30, 2023

**DOI:** 10.1002/ceat.202300256

## 1 Introduction

It is a well-known fact that exothermicity of chemical reactions may lead to instability in the form of self-sustained oscillations and/or multiple steady states (see e.g. [1]). Fundamental understanding is essential for process safety and process operation. To gain such a fundamental understanding, a continuous stirred tank reactor (CSTR) with an exothermic reaction of first order has been studied intensively in the past as a prototype system (see, e.g., [2] and references therein). It was shown that such a system is self-accelerating because the reaction rate increases with temperature leading to higher heat release by the chemical reaction, which in turn further accelerates the reaction, which may lead ultimately to instability.

In practice, the reaction mechanisms are often much more involved. Nevertheless, a similar thermokinetic self-acceleration can be observed in many practical systems. Typical examples are polymerization reactions [3], some homogeneously catalyzed liquid phase (e.g. [4,5]), and heterogeneously catalyzed gas phase reactions, like H<sub>2</sub> oxidation [6] or CO<sub>2</sub> methanation [7]. The latter has gained a lot of interest during the last years, in the framework of novel power-to-X concepts. In these concepts, green hydrogen is made by electrolysis using regenerative electrical energy. Afterward, hydrogen reacts with CO<sub>2</sub> from exhaust gases to methane [8].

The underlying reaction steps are similar to methanol synthesis, another exothermic heterogeneously catalyzed gas phase reaction representing another important candidate for the implementation of recent power-to-X concepts [8,9]. However, the dynamic behavior of methanol synthesis compared to the


methanation reaction seems to be entirely different and much more stable under the conditions commonly employed in practice. This is not only due to the fact that exothermicity is less pronounced compared to CO<sub>2</sub> methanation but also has to do with the temperature dependence of methanol formation, as will be shown in this paper.

For this purpose, in the next section some chemical details of both reaction systems are briefly reviewed and compared with each other. Afterward, a pseudo-homogeneous model of a CSTR is introduced for the theoretical analysis of the corresponding reaction systems. The final section presents selected results of a bifurcation and stability analysis of both systems and explains the main differences as indicated above.

## 2 Reaction Mechanism and Kinetics

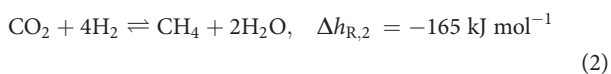
### 2.1 Methanation

Possible chemical reactions for the CO<sub>2</sub> methanation, also called Sabatier reaction, using Ni catalysts comprise [10]:

<sup>1</sup>Johannes Leipold  <https://orcid.org/0000-0002-1511-4794> (johannes.leipold@ovgu.de),

Dr.-Ing. Tobias Keßler, Prof. Dr.-Ing. Achim Kienle  
Otto-von-Guericke-University, Universitaetsplatz 2, 39106 Magdeburg, Germany.

<sup>2</sup>Magnus Jung, Prof. Dr.-Ing. Achim Kienle  
Max-Planck-Institut für Dynamik komplexer technischer Systeme,  
Sandtorstr. 1, 39106 Magdeburg, Germany.

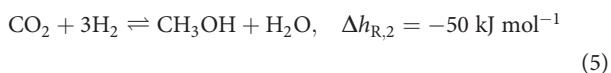
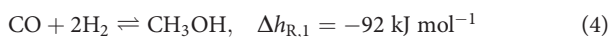


For simplicity, the reaction enthalpies  $\Delta h_{R,j}$  are considered to be constant in the remainder. Kinetics of methane steam reforming, i.e., the reverse Sabatier reaction, has been determined in [10] for a typical steam reforming catalyst with 15 wt % Ni/MgAl<sub>2</sub>O<sub>4</sub> under similar conditions employed in CO<sub>2</sub> methanation, i.e., pressures between 3 and 8 bar and temperatures between 300 °C and 400 °C. More recently, it was found that the kinetics also describes the Sabatier reaction reasonably well if a similar catalyst is used [11]. However, nowadays, more active catalysts with up to 50 wt % of Ni are employed for methanation, shifting CO<sub>2</sub> conversion temperature plots by about 50–100 °C to lower temperatures. For such more active catalysts a revised Langmuir Hinshelwood kinetics has been proposed in [12], which will be used in the present paper.

Further, it was argued, since CO formation via the reverse water-gas shift reaction (3) is endothermic, in principle, the amount of CO increases with rising temperature, but it was shown that the amount of CO is negligibly small at temperatures below 500 °C [7, 12], so that reactions (1) and (3) can be neglected for a pure H<sub>2</sub>/CO<sub>2</sub> feed. Another important aspect of CO<sub>2</sub> methanation is catalyst deactivation [13], which is, however, beyond the scope of this work and therefore not considered in this paper. An important aspect of CO<sub>2</sub> methanation, which is highly relevant for this paper and will be illustrated below, is the fact that CO<sub>2</sub> conversion, and therefore also the heat production of the chemical reaction, increases with rising temperature in the relevant range of operating conditions [7].

## 2.2 Methanol Synthesis

The focus in this paper is on methanol synthesis from synthesis gas using Cu/ZnO/Al<sub>2</sub>O<sub>3</sub> catalysts, which are routinely applied in industry. The reaction network comprises three main reactions, i.e., hydrogenation of CO and CO<sub>2</sub> as well as the water-gas shift reaction, according to:



Again, the reaction enthalpies  $\Delta h_{R,j}$  are considered constant. Typical operating conditions are pressures in the range of 50–60 bar and temperatures in the range of 250 °C. Under the standard conditions employed in industry, methanol formation proceeds mainly via CO<sub>2</sub> hydrogenation. Nevertheless, to over-

come the equilibrium limitation introduced by the formation of water during CO<sub>2</sub> hydrogenation, feed conditions including mainly CO are usually applied. This will 'bind' the water via the water-gas shift reaction, as CO is converted to CO<sub>2</sub> and further proceeds to methanol. However, the water-gas shift reaction is exothermic, and therefore the equilibrium shifts to the CO side as the temperature increases according to the principle of Le'Chatelier.

Hydrogenation of CO is much slower than hydrogenation of CO<sub>2</sub> and is often neglected. In this paper, all three reactions will be considered. Reaction kinetics were taken from our previous work [14, 15] with parameters from [16]. The kinetic model represents a Langmuir-Hinshelwood kinetics, with three different catalytically active centers, which are changing depending on the reductive/oxidative potential of the reaction gas. It was shown that this model provides very good agreement with a comprehensive set of 140 steady-state experiments and a series of dynamic experiments obtained by Vollbrecht in a micro-Berty type of reactor [17].

As shown above, methanol synthesis is also exothermic, but the reaction enthalpies are lower than for CO<sub>2</sub> methanation. But even more important is that the heat production of methanol synthesis is decreasing with increasing temperature in the relevant range of operating conditions usually employed in practice, leading to a completely different type of behavior, as will be shown below. This different type of behavior is mainly due to the temperature dependence of the reaction equilibrium of the water-gas shift reaction.

## 3 Mathematical Models

In the remainder, the classical analysis for a CSTR is extended with a simple first-order homogeneous exothermic reaction [18, 19] (see also [20] for a nice summary) to the present heterogeneously catalyzed multispecies multireaction systems described by Langmuir-Hinshelwood kinetics. The analysis is based on the following steady-state balance equation:

Component material balances:

$$0 = \dot{n}_{in} y_{i,in} - \dot{n} y_i + m_{cat} \sum_{j=1}^{N_r} \nu_{i,j} r_j(y, T, P), \quad i = 1, \dots, N_c \quad (7)$$

The total material balance is obtained from the component balances by summation over all species according to:

$$0 = \dot{n}_{in} - \dot{n} + m_{cat} \sum_{k=1}^{N_c} \sum_{j=1}^{N_r} \nu_{k,j} r_j(y, T, P) \quad (8)$$

and serves for the calculation of the molar flow rate at the outlet, which is different from the molar flow rate at the inlet due to the change of moles introduced by the chemical reactions (1)–(6). The energy balance reads:

$$0 = \dot{n}_{in} h_{i,in} - \dot{n} h_i - \dot{Q}_c \quad (9)$$

with the cooling rate  $\dot{Q}_c = kA(T - T_c)$ . The energy balance is reformulated by subtracting Eq. (7) multiplied with  $h_i$  and summed over all components from Eq. (9) resulting in a classical heat balance. If it is further assumed that the cooling

temperature  $T_c$  and the feed temperature  $T_{in}$  are equivalent, and the heat capacities  $c_{p,i}$  are constant, this heat balance reads:

$$0 = \underbrace{(\dot{n}_{in}c_{p,in} + kA)(T - T_c)}_{\text{heat removal } Q_{rm}} - \underbrace{m_{cat} \sum_{j=1}^{N_r} \Delta h_{R,j} r_j(y, T, P)}_{\text{heat production } Q_{pr}} \quad (10)$$

In these equations, the reaction rates depend on the composition of the reaction gas  $y$  and the temperature  $T$ . In the classical analysis for a first-order homogeneous chemical reaction, the material balance can be solved analytically for the concentration of the reactant and substituted into the heat balance, which then represents a single nonlinear equation for the temperature of the CSTR.

Steady-state solutions can be determined graphically by intersection of the sigmoidal heat production curve and the straight heat removal line (see, e.g., [20] for a detailed explanation). Multiple intersections represent multiple steady states. Static stability of these steady states can be determined from the slopes of the two curves at the intersection point. Static stability implies that after a small displacement from the steady state the system returns towards the steady state again. The more rigorous dynamic stability implies that the system will also settle down to the previous steady state again and may not oscillate around this steady state [19]. Static stability is a necessary but not sufficient condition for dynamic stability. Dynamic stability follows from the eigenvalues of the corresponding dynamic model equations [19].

The analysis can be extended to the considered heterogeneously catalyzed multicomponent multireaction systems. An analytical calculation of the heat production is not possible anymore, due to the highly nonlinear concentration and temperature dependence of the reaction rates. Instead, a semi-analytical approach is proposed, where the heat production is evaluated for different temperatures by a numerical solution of the material balances (7), (8) and substituting the solution into Eq. (9).

A similar approach was proposed by Bremer and Sundmacher [7] for the methanation reaction based on conversion rather than heat production. The present approach based on heat production is more suitable for multireaction systems like methanol synthesis but will be also applied to methanation to provide a direct comparison of the two reaction systems and elucidate the differences in behavior.

## 4 Results

### 4.1 Methanation

Results for methanation are presented in Figs. 1 and 2. Fig. 1 shows the methane yield of an isothermal CSTR as a function of temperature for a pressure of 5 bar and different residence times, as well as the

equilibrium yield. Since the temperature is below 800 K the reverse water-gas shift (RWGS) reaction was neglected as discussed above. This figure is equivalent to Fig. 1 in [7] but for consistency with the model equations introduced in the previous section, and the methanol synthesis to be discussed in the next paragraph employs a molar rather than a mass basis as in [7].

Fig. 2 displays the corresponding heat production curves  $Q_{pr}$  together with the heat removal curves  $Q_{rm}$ . The heat removal curves represent straight lines. The heat removal  $Q_{rm}$  is equal to zero at temperature  $T = T_c$ . The slope of this straight line lies between the vertical line (isothermal case) and the corresponding dashed line (adiabatic case for  $kA = 0$ ). It depends on the convective heat transport, given by the feed flow and the heat transfer to the cooling system, defined by the heat transfer coefficient and the transfer area  $kA$ . Steady-state solutions are the points of intersection between heat production and heat removal curves. From the geometry of the curves, it becomes obvious that up to three intersections are possible. The upper and the lower are statically stable according to the slope condition [18], whereas the intermediate is statically unstable, which is consistent with the observations in [7]. Parameters for methanation are summarized in Tab. 1.

**Table 1.** Parameters for methanation [7].

Parameter	Value	Units
$y_{CH_4,in}, y_{N_2,in}, y_{CO,in}$	0	[%]
$y_{CO_2,in}$	20	[%]
$y_{H_2,in}$	80	[%]
$P$	5	[bar]
$c_{p,in}$	30.69	[kJ kg <sup>-1</sup> K <sup>-1</sup> ]
$m_{cat}$	157	[g]
$A$	0.0187	[m <sup>2</sup> ]

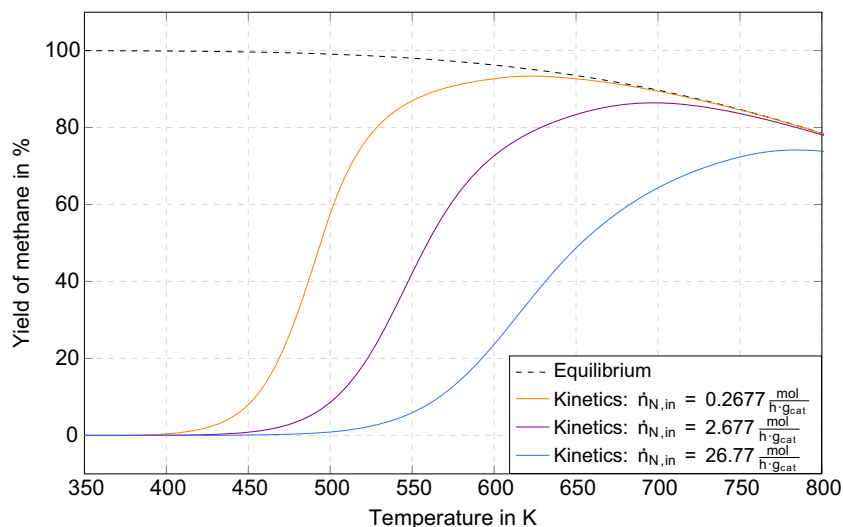


**Figure 1.** Yield of methane for different feed flow rates.

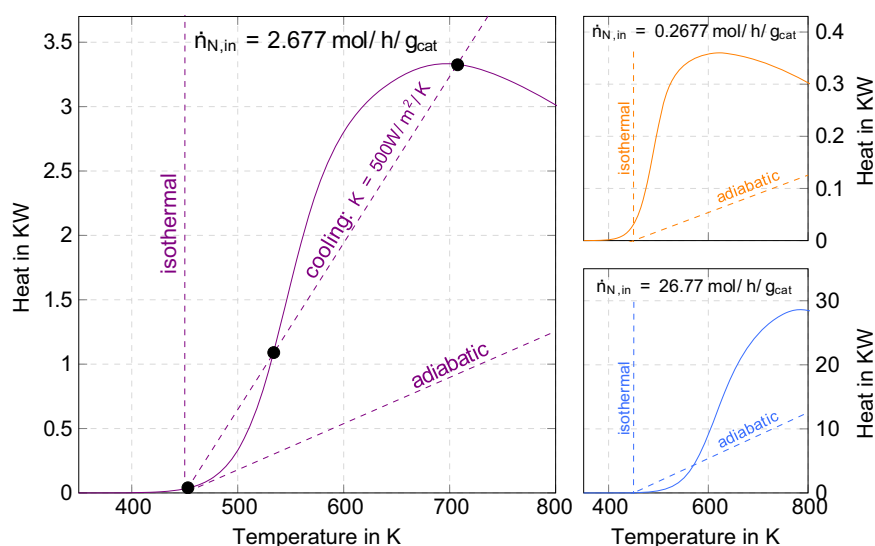


**Figure 2.** Heat production (solid) and heat removal (dashed) of  $\text{CO}_2$  methanation for different feed flow rates.

## 4.2 Methanol Synthesis

A completely different behavior is observed for methanol synthesis if the standard operating parameters are applied as summarized in Tab. 2. Here, a bell shape type of curve is observed for the methanol yield in Fig. 3, with a sharp increase at very low temperatures, a maximum and a sharp decrease at temperatures employed commonly in practice. Temperatures below 450 K are practically not relevant at this pressure because of possible condensation of the reaction products water and methanol [21, 22].

The methanol yield in Fig. 3 and the heat production curve in Fig. 4 have been calculated under the assumption of a homogeneous gaseous fluid phase, being therefore also rather hypothetical in this range. In practice, usually feed and cooling temperatures in the range of 500 K are employed. In this range, the heat production is decreasing with temperature. This is in contrast to the methanation reaction, where the heat production

**Table 2.** Parameters for methanol synthesis in a micro-Berty reactor [7].

Parameter	Value	Units
$y_{\text{CH}_3\text{OH},\text{in}}$	0.0	[%]
$y_{\text{CO}_2,\text{in}}$	2.1	[%]
$y_{\text{CO},\text{in}}$	18.5	[%]
$y_{\text{H}_2,\text{in}}$	64.4	[%]
$y_{\text{N}_2,\text{in}}$	15.0	[%]
$P$	50	[bar]
$c_{p,\text{in}}$	28.92	[kJ kg <sup>-1</sup> K <sup>-1</sup> ]
$m_{\text{cat}}$	3.95	[g]
$A$	0.0036	[m <sup>2</sup> ]

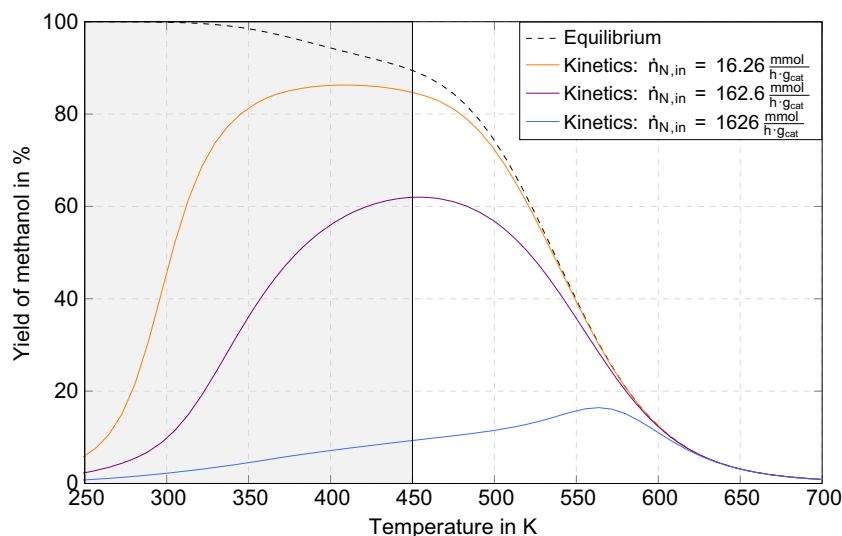


**Figure 3.** Yield of methanol for different feed flow rates.

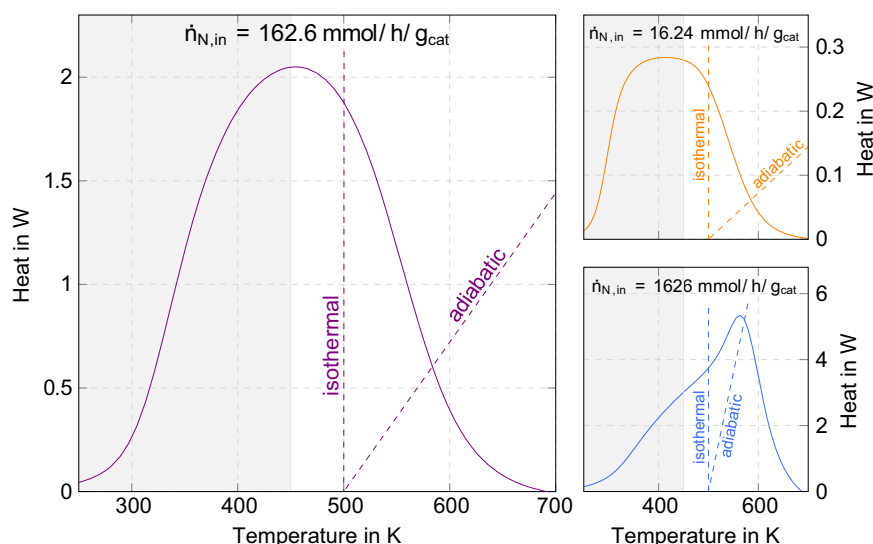


**Figure 4.** Heat production (solid) and heat removal (dashed) of methanol synthesis for different feed flow rates.

curve is increasing with temperature in the relevant range of operating conditions. This is mainly due to the temperature dependence of the water gas-shift reaction, which plays an important role in this system. Consequently, for operating conditions considered in this paper and commonly employed in practice, only a single intersection between heat production and heat removal curves is possible, corresponding to a unique and stable steady state.

For very large feed flow rates and thus for shorter residence times (as shown in Fig. 4 bottom right) and therefore with a lower yield of methanol (see Fig. 3), the behavior is slightly different. The heat production curve is increasing with temperature and the maximum is in the relevant range of operating conditions. However, due to the high flow rate, the heat removal through the convection term is also high, and thus the slope of the straight line is very steep. So, even in this case, there is only one point of intersection between the curves corresponding to a unique and stable steady state.

## 5 Conclusion

In this paper, it has been shown that methanol synthesis from synthesis gas in a CSTR with a standard Cu/ZnO/Al<sub>2</sub>O<sub>3</sub> catalyst will always have a unique and stable steady state under the typical operating conditions applied in current industrial practice. These comprise pressures in the order of 50–60 bar, feed, and cooling temperatures in the order of 500 K, and a feed composition with an over stoichiometric amount of H<sub>2</sub> and mainly CO as a carbon source. The main reason for this is that the heat production of the chemical reaction in contrast to the similar CO<sub>2</sub> methanation over Ni catalysts decreases with increasing temperature and is therefore not self-accelerating.

The situation may change if feeds with a higher amount of CO<sub>2</sub> are considered, which is of great interest to reduce greenhouse gas emissions. For this, however, different operating conditions and/or different catalysts are required, leading to diverse types of processes, which have now received a lot of attention in the recent literature [23, 24].

Nevertheless, the methodology developed in this paper could, in principle, also be used for these type of processes. For this, however, a new kinetic model is required accounting for the specific operating conditions and catalysts.

For simplicity, the focus in this paper was on a CSTR. As was shown in [7] for CO<sub>2</sub> methanation, the results can be directly extended to a cascade of CSTRs, which can be viewed as an approximation of a fixed-bed reactor, that is usually applied in industry.

## Data Availability Statement

Data available on request from the authors.

## Acknowledgment

Financial support by the German Research Foundation (DFG) is gratefully acknowledged for J. Leipold through the priority program SPP 2080 under grant KI 417/6-2 and for T. Keßler through the priority program SPP 2331 under grant KI 417/9-1. Open access funding enabled and organized by Projekt DEAL. [Correction added on 21 February 2024 after online publication: Equations 1, 2 and 3 are updated in this version.]

*The authors have declared no conflict of interest.*

## Symbols used

$A$	[m <sup>2</sup> ]	surface area
$c_p$	[J kg <sup>-1</sup> K <sup>-1</sup> ]	gas heat-capacity
$h$	[kJ]	enthalpy
$m$	[kg]	catalyst mass
$k$	[W m <sup>-2</sup> K <sup>-1</sup> ]	heat transfer coefficient
$\dot{n}$	[mol s <sup>-1</sup> ]	molar flow rate
$N_c$	[-]	number of components

$N_r$	[-]	number of reactions
$P$	[bar]	pressure
$Q$	[J s <sup>-1</sup> ]	heat rate
$r$	[mol s <sup>-1</sup> kg <sub>cat</sub> <sup>-1</sup> ]	reaction rate
$T$	[K]	temperature
$y$	[-]	mole fraction

### Subscripts

c	cooling
cat	catalyst
$i$	component
in	inlet
$j$	reaction
N	normalized on catalyst mass
pr	production
rm	removal

### Abbreviations

CSTR	continuous stirred tank reactor
RWGS	reverse water-gas shift

### References

- [1] L. F. Razon, R. A. Schmitz, *Chem. Eng. Sci.* **1987**, *42* (6), 1005–1047. DOI: [https://doi.org/10.1016/0009-2509\(87\)80055-6](https://doi.org/10.1016/0009-2509(87)80055-6)
- [2] A. Uppal, W. Ray, A. Poore, *Chem. Eng. Sci.* **1974**, *29* (4), 967–985. DOI: [https://doi.org/10.1016/0009-2509\(74\)80089-8](https://doi.org/10.1016/0009-2509(74)80089-8)
- [3] W. H. Ray, C. M. Villa, *Chem. Eng. Sci.* **2000**, *55* (2), 275–290. DOI: [https://doi.org/10.1016/S0009-2509\(99\)00323-1](https://doi.org/10.1016/S0009-2509(99)00323-1)
- [4] H.-P. Wirges, *Chem. Eng. Sci.* **1980**, *35* (10), 2141–2146. DOI: [https://doi.org/10.1016/0009-2509\(80\)85038-X](https://doi.org/10.1016/0009-2509(80)85038-X)
- [5] K.-P. Zeyer, M. Mangold, T. Obertopp, E. D. Gilles, *J. Phys. Chem. A* **1999**, *103* (28), 5515–5522. DOI: <https://doi.org/10.1021/jp990710v>
- [6] H. Beusch, P. Fieguth, E. Wicke, *Chem. Ing. Tech.* **1972**, *44* (7), 445–451. DOI: <https://doi.org/10.1002/cite.330440702>
- [7] J. Bremer, K. Sundmacher, *Front. Energy R.* **2021**, *8*. DOI: <https://doi.org/10.3389/fenrg.2020.549298>
- [8] R. Schlögl, *Angew. Chem. Int. Ed.* **2015**, *54* (15), 4436–4439. DOI: <https://doi.org/10.1002/anie.201405876>
- [9] G. A. Olah, *Angew. Chem. Int. Ed.* **2005**, *44* (18), 2636–2639. DOI: <https://doi.org/10.1002/anie.20046212>
- [10] J. Xu, G. F. Froment, *AIChE J.* **1989**, *35* (1), 88–96. DOI: <https://doi.org/10.1002/aic.690350109>
- [11] D. Schlereth, O. Hinrichsen, *Chem. Eng. Res. Des.* **2014**, *92* (2), 702–712. DOI: <https://doi.org/10.1016/j.cherd.2013.11.014>
- [12] F. Koschany, D. Schlereth, O. Hinrichsen, *Appl. Catal., B* **2016**, *181*, 504–516. DOI: <https://doi.org/10.1016/j.apcatb.2015.07.026>
- [13] S. Ewald, M. Kolbeck, T. Kratky, M. Wolf, O. Hinrichsen, *Appl. Catal., A* **2019**, *570*, 376–386. DOI: <https://doi.org/10.1016/j.apcata.2018.10.033>
- [14] C. Seidel, A. Jörke, B. Vollbrecht, A. Seidel-Morgenstern, A. Kienle, *Chem. Eng. Sci.* **2018**, *175*, 130–138. DOI: <https://doi.org/10.1016/j.ces.2017.09.043>
- [15] C. Seidel, A. Jörke, B. Vollbrecht, A. Seidel-Morgenstern, A. Kienle, *Chem. Eng. Sci.* **2020**, *223*, 115724. DOI: <https://doi.org/10.1016/j.ces.2020.115724>
- [16] C. Seidel, D. Nikolić, M. Felischak, M. Petkovska, A. Seidel-Morgenstern, A. Kienle, *Processes* **2021**, *9* (5), 872. DOI: <https://doi.org/10.3390/pr9050872>
- [17] B. Vollbrecht, Zur Kinetik der Methanolsynthese an einem technischen Cu/ZnO/Al<sub>2</sub>SO<sub>3</sub>-Katalysator, *Ph.D. Thesis*, Otto-von-Guericke University Magdeburg **2007**.
- [18] C. van Heerden, *Ind. Eng. Chem.* **1953**, *45* (6), 1242–1247. DOI: <https://doi.org/10.1021/ie50522a030>
- [19] E. D. Gilles, H. Hofmann, *Chem. Eng. Sci.* **1961**, *15* (3–4), 328–331. DOI: [https://doi.org/10.1016/0009-2509\(61\)85038-0](https://doi.org/10.1016/0009-2509(61)85038-0)
- [20] B. W. Bequette, *Process Dynamics – Modeling, Analysis and Simulation*, 1st ed., Prentice Hall PTR, Englewood Cliff, NJ **1998**.
- [21] A. Mirvakili, M. R. Rahimpour, *Appl. Therm. Eng.* **2015**, *91*, 1059–1070. DOI: <https://doi.org/10.1016/j.applthermaleng.2015.08.067>
- [22] K. Stangeland, M. H. Li, Z. Yu, *Ind. Eng. Chem. Res.* **2018**, *57* (11), 4081–4094. DOI: <https://doi.org/10.1021/acs.iecr.7b04866>
- [23] W. Bowker, *ChemCatChem* **2019**, *11* (17), 4238–4246. DOI: <https://doi.org/10.1002/cctc.201900401>
- [24] R. Guil-López, N. Mota, J. Llorente, E. Millán, B. Pawelec, J. L. G. Fierro, R. M. Navarros, *Materials* **2019**, *12* (23), 3902. DOI: <https://doi.org/10.3390/ma12233902>